

# Simple model of Lower Mississippi River backwater ecological function

**F. Douglas Shields, Jr.** Hydraulic engineer, cbec eco engineering, University, Mississippi, [d.shields@cbecoeng.com](mailto:d.shields@cbecoeng.com)

**William B. Rossell**, Doctoral Candidate, National Center for Computational Hydroscience and Engineering, University of Mississippi, University, Mississippi, [wrossell@ncche.olemiss.edu](mailto:wrossell@ncche.olemiss.edu)

**Clifford A. Ochs**, Professor, Department of Biology, University of Mississippi, University, Mississippi, [byochs@olemiss.edu](mailto:byochs@olemiss.edu)

## Abstract

Floodplain waterbodies (backwaters) comprise a critical component of large alluvial river ecosystems when they are intermittently connected to the main channel. This study investigated potential ecological benefits and impacts of the floodplain area between the mainline levees and specifically, backwaters along the Lower Mississippi River (LMR) regarding downstream flux of nutrients and chlorophyll-a. To assess these ecological responses, we developed a simple model of a hypothetical LMR reach for interactions between the main channel and backwaters under a range of hydrologic conditions. The spatial domain of the model is a single hypothetical backwater and an associated main channel reach. Nutrient and chlorophyll-a concentrations are based on water quality data obtained from a 28-km reach of the LMR over the last 15 years. Water movement is simulated using relationships developed using upstream gage records, site water level data, and the Adaptive Hydraulics Modeling System (AdH) simulations. Simulations of backwater performance using hydrologic records for 1992-2021 and a range of geometries typical of four prototypes within our study reach indicated an average of 0.14% to 2.6% of the annual main channel flow passed through one of the four backwaters. The total effect of the four backwaters over the 29-year period was to retain 0.34% and 0.39% of the main channel loads of nitrate and phosphate, respectively. Mean backwater production of algal biomass ranged from 13.3 to 37.1 kg chlorophyll-a/ha/yr, while retention of nitrate ranged from 1,700 to 3,150 kg/ha/yr and phosphate retention ranged from 57 to 146 kg/ha/yr. Simulations of performance of a hypothetical backwater for 1992-2021 and a range of hydrologic connectivity indicated average flow diversion, backwater nitrate and phosphate retention were inversely related to the river stage required for main channel connection to the backwater, while chlorophyll-a contribution was directly related to controlling stage. Reducing the controlling elevation for hydrologic connection by 10 m increased average nitrate and phosphate retention per unit area by factors of about 4 and 9, respectively. The model presented here should enable determinations of backwater effects on the main channel flux of nitrate, phosphate and chlorophyll-a for a range of backwater geometries and over any temporal domain within the period of record for the Helena, Arkansas gage (1871-present).

## Introduction

This paper applies to the Lower Mississippi River (LMR) section between Cairo and Baton Rouge, where the river has a substantial remnant floodplain between bluffs and levees (Biedenharn et al. 2018). The LMR main channel (MC) and floodplain backwaters (BWs) display substantial seasonal variation in inundated area and connectivity (Baker et al. 1991). During the typical spring high water period, the entire region between the flood control levees (or, in some cases bluffs) may be inundated, which is roughly 1.5 to >10 times wider than the MC base flow

width. BWs and riparian areas may remain flooded for two or more months before the river recedes (Schramm et al. 2009). As river stage declines in summer, MC width, depth, and discharge decline, resulting in increased disconnection between the MC and floodplain BWs as previously flooded riparian areas transition to terrestrial habitat.

## **Backwaters**

As a result of an extensive levee system, only about 10-20% of the historical floodplain remains seasonally connected to MC flow (Baker et al. 1991). The remnant connected floodplain ranges in width from 0.1 to 10 km. Depending on the river stage, about 116,000 and 707,000 ha of off-channel floodplain aquatic habitat remains, including ~1,600 lakes, and various other seasonally inundated features such as bottomland hardwood forest (Baker et al. 1991; Hartfield 2014). LMR off-channel aquatic habitats may be classified in various ways (e.g., Baker et al. 1991, Shields 1995, Miranda et al. 2021). Aquatic habitats include natural features such as abandoned channels, sloughs, oxbow lakes and secondary channels, and manmade features such as dike field pools, borrow pits and secondary channels modified by river training dikes. Cutoff meander bends are significant BW habitats that have resulted from natural and anthropogenic processes and are characterized by blockage and infilling of MC connections (Gagliano and Howard 1984, Shields and Abt 1989). Bars of bed material are deposited in the downstream channel more slowly than for the upstream entrance, resulting in a narrow downstream "tie" channel that provides continuous or periodic hydrologic connection to the MC (Shields and Abt 1989, Rowland et al. 2005). Until completely filled with sediment, tie channels are an important passageway for water and dissolved and particulate materials moving between the MC and BW.

## **Nutrients and phytoplankton**

The dynamic hydrology of the LMR regulates variation in ecological and biogeochemical processes across the floodplain and down the river corridor (Junk et al. 1989; Scott et al. 2014) and nutrient loading from the LMR ensues a cascade of biological production, food web interactions, and biogeochemical transformations (Pongruktham and Ochs 2015). The LMR transports enormous quantities of nitrogen and phosphorus to the Gulf of Mexico, (Goolsby et al. 1999), and both nutrients appear to be a contributing factor in northern Gulf of Mexico hypoxia (Laurent and Fennel 2014).

The effect of BWs on LMR nitrogen flux is of particular interest because of its role as a pollutant promoting primary production which leads to estuarine hypoxia in the Gulf of Mexico (Goolsby et al. 1999, Tian et al. 2020). Trends for the MC upstream of the Old River Control Structure (located between Natchez, MS and Baton Rouge, LA) from 1975-2017 indicate increasing total N (+18%) and increasing nitrate plus nitrite ( $\text{NO}_2 + \text{NO}_3$ , +29%) (Stackpole et al. 2021). In the LMR MC, there appears to be little net removal of N (Alexander et al. 2000; Coupe et al. 2013; but see Strauss et al. 2011) because (except during extreme low flow) the channel is well-mixed, highly oxygenated, and turbid, all of which can inhibit nitrogen loss through denitrification and primary production (Ochs et al. 2013). However, conditions are sometimes much more favorable for denitrification and primary production in floodplain BWs (Pongruktham and Ochs 2015).

With regards to P transport in the LMR, generally large rivers are less retentive of P than smaller streams due to a higher ratio of water volume to bed sediment, poorer light penetration, and relative scarcity or absence of benthic algae, periphyton, and macrophytes (Withers and Jarvie 2008). Regardless of stream size, P availability is governed by complex geochemical processes which affect its affinity for absorption and desorption to and from clay-rich particles (including both benthic and suspended sediments) into water. Phosphorus moves from

sediment into solution in the water column or vice versa due to geochemical processes resulting from the overall chemical environment; however, oxygen concentration is a primary factor in the absorption vs. desorption process (Evans et al. 2021). Because of the tendency for P to sorb to benthic sediments, wetland sediments can be a long-term sink for P storage but recent evidence specific to this region suggest that P can also be transported from reduced sediment to shallow groundwater (Justus 2022). Dissolved orthophosphate as P ( $\text{PO}_4\text{-P}$ ) can also be assimilated by phytoplankton, terrestrial vegetation, and microorganisms. The length of time P is stored by different organisms can vary widely depending on biotic materials' life cycle and fate (Wohl 2021).

As floodwaters enter a BW, flow velocities generally decrease, and suspended sediments settle out, reducing turbidity in the photic zone where a majority of biological uptake occurs and chlorophyll is produced. Once turbidity is reduced in floodplain BWs to the point that algal productivity occurs,  $\text{PO}_4\text{-P}$  is often consumed to below detection during and after phytoplankton blooms (Pongruktham and Ochs 2015). Phytoplankton and associated chlorophyll produced in BWs is conveyed back to the MC due to hydrologic connection, potentially intensifying riverine secondary production (Cloern 2007; Eckblad et al. 1984). Essentially, in exchange for nutrients provided by the MC, BW-produced biomass subsidizes the MC ecosystem.

Phytoplankton biomass flux is of interest because of its potential contribution to the food web of the light-limited MC. Phytoplankton production in the MC is light-limited due to high turbidity generally resulting from suspended sediment. Chlorophyll-a concentration is used in the model described herein as a surrogate for phytoplankton. BW chlorophyll-a levels may be temporally light-limited when BWs are strongly connected to the turbid MC but can switch to being nutrient-limited following hydrologic disconnection, subsequent improved water clarity and resulting phytoplankton blooms. As the river falls from May-August, MC chlorophyll-a levels typically remain low (6-8  $\mu\text{g/L}$ ), but concentrations in the BW can increase to values > 300  $\mu\text{g/L}$ .

## Field data

The model described herein was developed using field data collected from a 28-km reach of the LMR south of Tunica, Mississippi (Ochs et al., 2013; Pongruktham and Ochs 2015). Within this reach, we sampled the MC and four BW sites. The BW sites included a secondary channel partially blocked at the upstream end by a notched stone dike (Quapaw), a slough (Modoc), and two oxbow lakes (Mellwood and Desoto) formed by a manmade cutoff in the early 1940s (**Table 1**).

### Water quality and algal biomass

Empirically derived variables used to parameterize the model were derived from laboratory analyses of samples collected from these sites between 2007 and 2017. BW dissolved nutrient and chlorophyll-a concentrations were based on values for water and plankton samples collected in triplicate at approximately 0.5-m depth within the BWs or near the center of the MC. Detailed description of sample sites and research methods can be found in Pongruktham and Ochs (2015).

### Water levels

A network of Onset pressure transducer-type self-contained logging water level recorders was deployed in 2021 at selected locations within the MC and BWs in the study reach. Datums for

water level recorders were established by surveying the water surface elevation at each installation site using a Topcon GR3 real-time kinematic global positioning system. Datums were accurate within 0.02 m, and the loggers recorded water depth within 0.1% of the measured value. Water depths were corrected for barometric pressure variations by subtracting the barometric pressure measured at reference loggers placed in the air adjacent to the study sites. We also used water level data from the Helena, Arkansas gage (USGS 07047970 and USACE MS 133), located 34 km upstream from our study reach.

**Table 1.** Geometric characteristics of Lower Mississippi River study backwaters. Length and width are nominal values measured from recent aerial photographs taken at baseflow.

Backwater	Type	Length km	Mean width m	Surface area ha	Controlling Helena gage height <sup>1</sup> m	Controlling water surface elevation m NAVD88
Quapaw	Secondary channel	9	159	143	1.7	41.9
Modoc	Slough	4	154	61	9.0	49.1
Mellwood	Cutoff meander bend	9	324	292	10.1	49.1
Desoto	Cutoff meander bend	12	611	509	10.0	48.6
BW <sub>h</sub>	Hypothetical	7.5	514	386	varies	varies

## Model

We built a simple model that simulates the effect of a hypothetical backwater on the overall flux of NO<sub>3</sub>-N, PO<sub>4</sub>-P and chlorophyll-a in the LMR. The spatial domain of the model comprises two compartments: a single hypothetical backwater (BW<sub>h</sub>) and an associated MC reach. Water movement is simulated using relationships developed using upstream gage records, site water level data, and the Adaptive Hydraulics Modeling System (AdH) simulations. Using the model, impacts of BW<sub>h</sub> on downstream flux of NO<sub>3</sub>-N, PO<sub>4</sub>-P, and chlorophyll-a may be simulated for a range of backwater geometries and over any temporal domain within the period of record for the Helena, Arkansas gage (1871-present). PO<sub>4</sub> simulations are limited to the periods beginning later than April 1991 due to the unavailability of required daily MC water temperature data for earlier dates.

### Water movement

Water level data from our study sites showed a tight linkage between MC and BW<sub>h</sub> stages. BW<sub>h</sub> stage tends to mirror MC stage closely but lags by a few hours. The relationship between MC and BW is interrupted only during shallow river stages when the channel stage falls below the level at which MC and BW<sub>h</sub> are hydrologically connected. Below this level, the BW<sub>h</sub> water level stabilizes or falls more slowly.

**Main channel velocity:** The model runs on an hourly timestep and accepts daily river stage,  $z$  [m] as input. MC stage at the upstream end of BW<sub>h</sub> is represented by records from the

---

<sup>1</sup> Stage on Mississippi River gage at Helena, AR at which water from river enters backwater via the upstream tie channel. Values shown are based on field observations of backwater conditions and concurrent stages at Helena. Detailed analysis by Oliver (A. Oliver, PowerPoint file, "Mississippi River GIS analyses, 13 July 2021) indicated Quapaw was barely disconnected on June 24, 2012, with a local water surface elevation of 41.2 m. The Helena gage reading at 8:00 a.m. local time on that date was 1.13 m (rivergages.com).

Mississippi River at Helena, Arkansas, gage. Discharge,  $Q$  [ $\text{m}^3/\text{s}$ ] is computed from stage using a rating curve provided by the USACE Memphis District. As a check on assumptions used in developing the water quantity algorithm (described below), reach-mean velocity,

$V_{MC}$  [ $\text{m}/\text{s}$ ], for the MC is computed at each timestep using a hydraulic geometry relation:

$$V_{MC} = k(Q - Q_u)^m \quad (1)$$

in which  $Q_u$  [ $\text{m}^3/\text{s}$ ] is the discharge exiting the MC and entering  $BW_h$  through the upstream linking channel. Default values used by the model for  $k$  and  $m$  in **Equation 1** are 0.0180 and 0.453, respectively. These values are consistent with published values for meandering sand bed rivers (Richards 1982) and produce velocities comparable with measurements obtained by the USGS at LMR gaging stations between Memphis and Natchez (from USGS 2022).

**Flow into backwater:** From field observations and simulation models (Howe and Gaines 2017), flow into and through  $BW_h$  occurs when the MC exceeds some critical level,  $z_{crit}$ , which is shown in the next to the last column of **Table 1**. At lower river stages ( $z < z_{crit}$ ) flow in the upstream tie channel,  $Q_u$  [ $\text{m}^3/\text{s}$ ] = 0. In the model, discharge from MC into  $BW_h$  through the upstream channel at each timestep is given by a power function:

$$Q_u = a(z - z_{crit})^b \quad (2)$$

for  $z - z_{crit} > 0$ , and

$$Q_u = 0 \quad (3)$$

for  $z - z_{crit} \leq 0$ .

The former condition is referred to herein as "connected," while the latter is "isolated." The form of **Equation 2** and the range of typical values for the coefficients  $a$  and  $b$  were determined by fitting curves to output from numerical simulations of the study reach for calendar years 2008 and 2011 performed by G. Savant using the AdH hydrodynamic model (Howe and Gaines 2017) (**Table 2**). Coefficients and exponents in **Table 2** reflected  $z_{crit}$  values and local floodplain topography.

**Table 2.** Nonlinear regression values ( $y = ax^b$ ) for the difference between river stage and critical level ( $x = z - z_{crit}$ ) and flow from the MC into the backwater ( $y = Q_u$ ). Data obtained from simulations of 2008 and 2011 calendar year flows using AdH model of study reach.

Backwater	Coefficient, a	Exponent, b	$r^2$
Quapaw	57.60	1.32	0.886
Modoc	31.10	1.96	0.998
Mellwood	15.60	2.64	0.973
Desoto	80.05	2.47	0.997
Default for $BW_h$	50.00	2.50	n/a

**Flow out of backwater:** The flow in the  $BW_h$  downstream tie channel,  $Q_d$ , may be positive (toward the MC) or negative (toward  $BW_h$ ) and is computed based on mass balance:

$$Q_d = \left( Q_u - \frac{\Delta V}{\Delta t} \right) \quad (4)$$

In which  $\Delta V$  is the change in the volume of water in  $BW_h$ ,  $Vol_{BW}$ , during the timestep in question, and  $\Delta t$  is the length of the timestep (1 hr). The change in BW volume is given by:

$$\Delta V_t = Vol_{BW_t} - Vol_{BW_{t-1}} \quad (5)$$

BW volume is computed at each timestep as the product of the mean width,  $W_{BW}$ , mean depth,  $D_{BW}$ , and  $BW_h$  length,  $L_{BW}$ :

$$Vol_{BW} = W_{BW} D_{BW} L_{BW} \quad (6)$$

The user specifies BW length (limited to values between 300 and 30,000 m) and is assumed to be invariant with time and fluctuating river stage. The mean BW water width and depth are computed at each timestep as functions of the Helena gage height:

$$W_{BW} = \max(W_{min}, az_H^b) \quad (7)$$

$$D_{BW} = \max(D_{min}, cz_H) \quad (8)$$

in which  $z_H$  is hourly Helena gage height,  $W_{min}$  and  $D_{min}$  are minimum BW mean water width and depth, and  $a$ ,  $b$  and  $c$  are parameters which users may modify.

When the river falls, hydraulic connection between most LMR BWs and the MC via the downstream tie channel persists even after  $BW_h$  is in the "isolated" state. The discharge through the downstream tie channel,  $Q_d$  [m<sup>3</sup>/s], is gradually-varied open channel flow, but data and hydrodynamic simulations available for this study were not adequate to fully characterize these flows. Furthermore, the data extracted from AdH simulations used to produce the values shown in **Table 2** were limited to major flow events, as data from smaller events tended to contain noise and unrealistic values for BW stage and flow. However, we assess that these model realism shortcomings do not significantly affect overall BW impacts to river nutrient and chlorophyll flux. Visual observations and data from water level recorders suggest that, during river stages lower than  $z_{crit}$ , flows move alternately in and out in the downstream tie channel. Simulation using **Equation 4** reproduced this bidirectional flow in the downstream tie channel. Flow through the downstream channel is efficient enough to maintain BW levels so that there is little difference between river and BW stages until the river drops so low that flow through the downstream tie channel ceases.

**Backwater velocities:** To check assumptions used in developing the water movement algorithm, reach-mean velocities for  $BW_h$  are computed at each timestep whenever  $Q_{u_t} > 0$ . The ideal hydraulic retention time for water passing through  $BW_h$  is computed at each timestep for which  $Q_{u_t} > 0$  by dividing the water volume by the average of the discharges in the upstream and downstream linking channels. The actual hydraulic retention time,  $HRT_{BW}$ , is given by multiplying ideal retention time by an efficiency factor of 0.75 (Thackston et al. 1987):

$$HRT_{BW} = \frac{0.75 Vol_{BW}}{(Q_u + Q_d)/2} \quad (9)$$

The mean BW velocity,  $V_{BW}$  [m/s], is computed at each timestep:

$$V_{BW} = \frac{L_{BW}}{HRT_{BW}} \quad (10)$$

Observations of LMR BWs indicate that current velocities are negligibly small at river stages too low to produce significant flows through the BW. BW flow velocities gradually increase at higher

stages to approach MC velocities during the very highest flows. Users may plot model output velocity time series to verify that this behavior is replicated.

## Water quality and algal biomass

The model computes the concentrations of NO<sub>3</sub>-N, PO<sub>4</sub>-P and chlorophyll-a in the MC at the upstream and downstream ends of the spatial domain and within BW<sub>h</sub>. BW<sub>h</sub> is assumed to be completely mixed; although longitudinal, lateral and vertical variations in BW quality exist at times, they are ignored. Concentrations are computed using empirical formulas developed using our data and, in some cases, data collected and published by the USGS. Measured data used to parameterize the model include river stage and measured MC and BW dissolved nutrient and chlorophyll-a concentrations (e.g., Pongruktham and Ochs 2015). Model default values for the formula coefficients and exponents are based on regression analyses of our field data. The user may modify default values prior to each run.

**Main channel:** Field data from our collections and the USGS were used to develop empirical relations for MC nutrient and chlorophyll-a concentrations. Nitrate concentration in the MC is computed using a regression based on Julian date and river stage.

$$[NO_3 - N]_{MC} = 0.701(z_H / z_{max}) + 0.00396AJD + 0.843 \quad (11)$$

in which  $[NO_3 - N]_{MC}$  represents the nitrate concentration in the upstream end of the simulated reach in mg/L as N, AJD represents the Julian date adjusted by advancing 150 days<sup>2</sup>, and  $z_H / z_{max}$  represents the river stage divided by the maximum recorded stage (18.35 m). This relation produces NO<sub>3</sub> -N concentrations ranging from about 1.0 to about 2.5 mg/L, while concentrations in our data set span nearly 0.0 to 3.7 mg/L. High-frequency measurements by the USGS for the LMR MC at Vicksburg (2013-2021) and Baton Rouge (2011-2021) indicate NO<sub>2</sub> + NO<sub>3</sub> levels in the range of 0.22 to 3.1 mg/L (as N). However, the **Equation 11** does reproduce the central trend of our data well.

MC PO<sub>4</sub>-P concentration is computed using a regression formula with river water temperature as the independent variable:

$$[PO_4 - P]_{MC} = 0.0000977T^2 - 0.0017956T + 0.069004 \quad (12)$$

in which  $[PO_4 - P]_{MC}$  is the MC PO<sub>4</sub>-P concentration in mg/L and T is the daily LMR water temperature. This relationship reflects seasonal variations in MC PO<sub>4</sub>- P levels and, perhaps, the effects of water temperature on PO<sub>4</sub>-P solubility. Long-term, daily records of other water quality variables that usually co-vary with PO<sub>4</sub>-P (e.g., suspended sediment or turbidity) were not available.

The model uses water temperatures recorded by the USGS gage at Baton Rouge, Louisiana (Site No. 07374000) because of its length of record (1991-present). The model predicts MC PO<sub>4</sub>-P values based on the historical temperature record with gaps filled using a sinusoidal curve fit to the available data:

---

<sup>2</sup> For example, the Julian date for April 1 is 91 as it is the 91st day of the calendar year. The adjusted Julian date would be 91 + 150 = 241. For December 1, 336 + 150 = 486, but since Julian date cycles on 365, the adjusted date would be 486 - 365 = 121.

$$T(t) = 12.513 \sin\left(\frac{2\pi}{8766}(t - 511.053)\right) + 18.519 \quad (13)$$

in which  $t$  is the time in hours since midnight, April 11, 1991. **Equation 12** produced MC PO<sub>4</sub>-P values between about 0.06 to 0.12 mg/L for 1992-2021. Measurements in our data set span 0.04 to 0.14 mg/L.

MC chlorophyll-a concentration at the upstream end of the simulated reach,  $CHL_{MC_{ups}}$  [µg/L], is computed at each timestep using a quadratic function fit to our field data using nonlinear regression:

$$CHL_{MC_{ups}} = 0.0283z_H^2 - 1.0865z_H + 13.643 \quad (14)$$

in which  $z_H$  is the gage height [m] at Helena, Arkansas. **Equation 14** produces values of  $CHL_{MC_{ups}}$  ranging from 3.2 µg/L to 14.7 µg/L for the historical maxima and minima of  $z_H$ , respectively. The observed values in our data set lie between 1.1 µg/L and 24 µg/L.

**Backwater:** BW water quality constituent concentrations are estimated using empirical relations fit to field data. When BW<sub>h</sub> has hydraulic connection to the MC ( $z_H - z_{crit} > 0$ ), the ratio of BW to MC concentration approaches 1.0 as river stage increases and more flow enters BW<sub>h</sub>. Specific forms and parameters for the empirical relations for connected BW water quality are provided in **Table 3**.

**Table 3.** Formulas for water quality constituents in backwaters with upstream hydraulic connection to the MC ( $z_H - z_{crit} > 0$ ). Here  $y$  = BW concentration/MC concentration and  $x = z_H - z_{crit}$ ,  $t$  is time in hours, and MAE = mean absolute error.

Constituent	Range of applicability	Form of relation	Coefficient a	Coefficient b	R <sup>2</sup>	MAE
NO <sub>3</sub> -N, mg/l	$z_H - z_{crit} > 0.1 \text{ m}$	$y = \min[1.0, a*\ln(x) + b]$	0.1371	0.7346	0.425	0.150
	$0 < z_H - z_{crit} \leq 0.1 \text{ m}$	Falling stage, $y = a$ Rising stage, $y(t) = y(t-1)$	0.430	n/a		
PO <sub>4</sub> -P, mg/l	$z_H - z_{crit} > 0.1 \text{ m}$	$y = \min[1.0, a*\ln(x) + b]$	0.1128	0.7656	0.690	0.053
	$0 < z_H - z_{crit} \leq 0.1 \text{ m}$	Falling stage, $y = a$ Rising stage, $y(t) = y(t-1)$	0.510	n/a		
Chlorophyll-a, µg/l	$z_H - z_{crit} > 1 \text{ m}$	$y = 1 + ae^{bx}$	20	-2.5	0.469	2.27
	$0 < z_H - z_{crit} \leq 1 \text{ m}$	$y(t) = y(t-24\text{hr})$	n/a			

When river stage  $z_H$  falls below the critical level for hydrologic connection via the upstream tie channel,  $z_{crit}$ , concentrations are a function of the duration of hydraulic isolation,  $i$ , measured in days. NO<sub>3</sub>-N concentrations fall with increasing duration of isolation presumably due to gradual depletion of the available N by biological uptake, microbial action and denitrification. Similarly, PO<sub>4</sub>-P concentrations gradually fall, presumably due to biological uptake and physical processes. In contrast to the decline in nutrient concentrations with isolation time, chlorophyll-a levels increase with time when river stage falls and BW isolates ( $z_H - z_{crit} < 0$ ) until algal populations begin to exhaust the available nutrients. Our observations indicate that after about 40 days of continuous hydrologic isolation,  $CHL_{BW}$  gradually declines with time. Specific forms and parameters for the empirical relations for isolated BW water quality are provided in **Table 4**.



**Table 4.** Formulas for water quality constituents in isolated backwaters ( $z - z_{crit} \leq 0$ ). Here  $y = (\text{BW concentration})/(\text{MC concentration at time of isolation})$  and  $x = \text{isolation time in days}$ . MAE = mean absolute error.

Constituent	Range of applicability	Form of relation	Coefficient a	Coefficient b	R <sup>2</sup>	MAE
NO <sub>3</sub> -N, mg/l	$0 < i \leq 425$	$y = \min[0.43, a \cdot \ln(x) + b]$	-0.086	0.521	0.192	0.164
	$i > 425$	$y = 0$				
PO <sub>4</sub> -P, mg/l	$0 < i \leq 216$	$y = \min[0.51, a \cdot \ln(x) + b]$	-0.148	0.796	0.156	0.228
	$i > 216$	$y = 0$				
Chlorophyll-a, mg/l	$i \leq 40$ days	$y = ae^{-bx}$	14.59	0.446	0.046	30.40
	$i > 40$ days	$y = a \cdot \ln(x) + b$	-17.14	143.05		

### Flux and load

Concentrations determined using formulas presented herein were combined with water flows to obtain mass fluxes into and out of BW<sub>h</sub> and MC. Flux values were multiplied by time step length to calculate loads, and loads were summed by year and for the entire model run (1992-2021).

## Analysis

Using the model, simulations of hypothetical BWs similar to the four study BW sites (**Table 1**) for the period calendar years 1992-2021 were completed. Then a series of 1992-2021 simulations were conducted for a fifth hypothetical BW with properties intermediate to the study sites, but varying connectivity ( $z_{crit}$  values). Mean rates of BW nutrient retention and chlorophyll-a contribution were computed by dividing net annual flux by median water surface area. Summary statistics were computed for nutrient and chlorophyll effects on the MC load by year and the entire simulation period.

## Simulation results

The 1992-2021 period selected for simulation included very wet and dry years. The range of annual average computed discharges at Helena and associated loads of nutrients and chlorophyll-a are presented in **Table 5**.

**Table 5.** Lower Mississippi River mean annual main channel flows and simulated mean annual nutrient loads and chlorophyll-a loads for the driest (2000) and wettest (2019) years during the period 1992-2021 and the means for that period.

Calendar year	Mean annual discharge (rank <sup>3</sup> )	Annual load of NO <sub>3</sub> -N, tonnes	Annual load of PO <sub>4</sub> -P, tonnes	Annual load of chlorophyll-a, tonnes
2000	10,900 (147)	621,000	26,500	3,480
2019	28,400 (1)	1,900,000	65,400	4,740
Mean 1992-2021	17,600 ± 3,700	1,080,000 ± 275,000	41,100 ± 8,840	4,020 ± 280

To highlight the response of model concentrations to discharge and seasonal influences, outputs for water years 2011-2012, which comprised extremely high and low flows, are presented in **Figures 1** and **2**. Symbols in **Figure 1** nutrient concentration plots represent concentrations measured by the USGS above Vicksburg (site no. 322023090544500) while symbols in the

<sup>3</sup> Rank of annual mean stage, Mississippi River at Helena for 1871-2020.

chlorophyll plot are measurements at Baton Rouge (Turner et al. 2022). Model concentrations are within ranges and display similar trends to the measured data, despite the differences

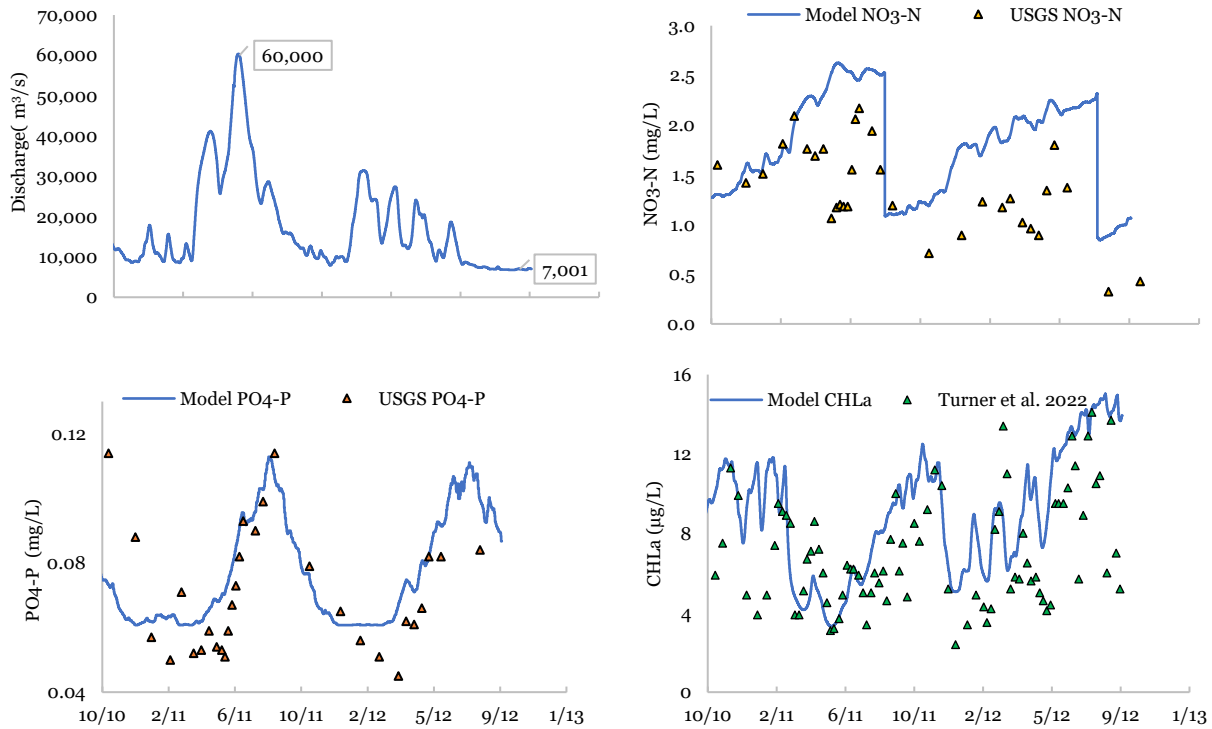


**Figure 1.** MC discharge and concentration hydrographs for the model reach, water years 2011-2012.

in discharge and contributing watershed between the study reach and sampled sites. Summary statistics for 1992-2021 BW influence on MC flows and loads of nutrients and chlorophyll-a are presented in **Table 6**. The total nutrient retention by the four study backwaters for 1992-2021 averaged about 3,700 tonnes/yr and 160 tonnes/yr for NO<sub>3</sub>-N and PO<sub>4</sub>-P, respectively, or about 0.34% and 0.39% of the MC load, respectively. Total chlorophyll-a contribution averaged about 36 tonnes/yr or about 0.9% of the MC load. NO<sub>3</sub>-N retention is lower than we computed with a previous version of our model (Ochs and Shields 2019) which was based on assumptions regarding water movement rather than field measurements and AdH simulations. Time series of simulated BW nutrient concentrations (**Figure 2**) indicate the sensitivity of these constituents to hydraulic connection, with much higher levels in the highly connected Quapaw secondary channel. Chlorophyll-a levels (**Figure 2**) were also sensitive to connecting flows but followed trends opposite the nutrients.

Connectivity between MC and BW governs nutrient retention, and the parameters of **Equation 2** ( $a$ ,  $b$  and  $Z_{crit}$ ) were key determinants of hydrologic exchange between the MC and BW. A series of 1992-2021 simulations of BW<sub>h</sub> with  $Z_{crit}$  varying between 2 m and 12 m indicated that average retention declined with increasing  $Z_{crit}$  while chlorophyll-a contribution increased (**Table 7**). Although there is likely covariation of  $a$ ,  $b$  and  $Z_{crit}$  in prototype LMR BWs, the **Table 7** simulations were based on varying only  $Z_{crit}$ . Plots of annual NO<sub>3</sub>-N retention versus annual mean discharge for a range of  $Z_{crit}$  values (**Figure 3**) show that the relationship between retention and mean annual discharge is increasingly noisy and nonlinear with greater connectivity (decreasing  $Z_{crit}$ ).

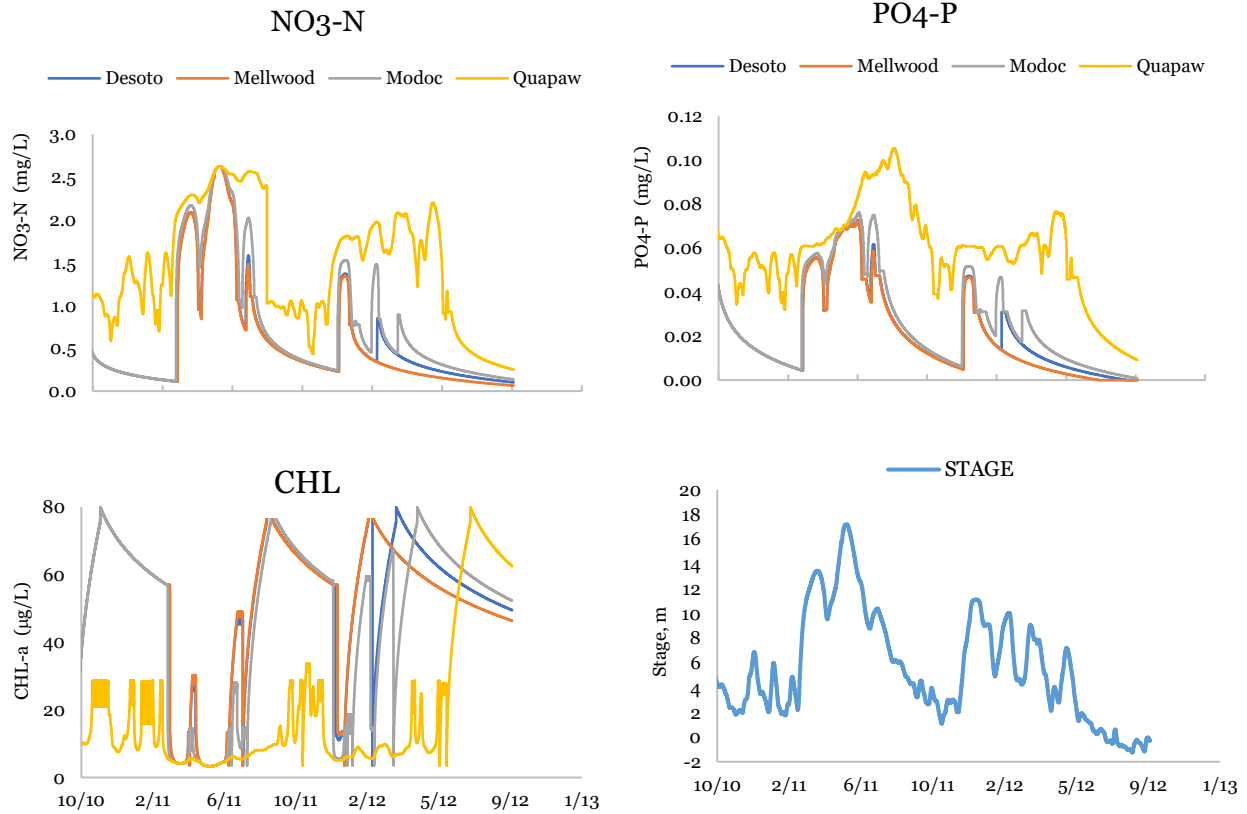


**Figure 2.** Concentration hydrographs for four simulated backwaters (described in **Tables 1** and **2**), and MC stage, water years 2011-2012

**Table 6.** Mean percent of MC flow passing through BW, annual nutrient retention, and chlorophyll-a contribution for individual hypothetical Lower Mississippi River backwaters with geometries similar to study backwaters listed in **Table 1**.

Model backwater similar to	Mean % of MC flow passing through BW	Mean retention of NO <sub>3</sub> -N, kg/ha/yr	Mean retention of PO <sub>4</sub> -P, kg/ha/yr	Mean contribution of chlorophyll-a, kg/ha/yr
Quapaw	2.63	2,530	146	13.3
Modoc	0.256	3,150	108	25.0
Mellwood	0.144	1,700	57	37.1
Desoto	0.644	1,320	60	8.7

**Table 7.** Mean percent of MC flow passing through BW, annual nutrient retention, and chlorophyll-a contribution for hypothetical Lower Mississippi River backwaters with geometry intermediate to study backwaters listed in **Table 1**.

$Z_{crit}$ , m	Mean % of MC flow	Mean retention of NO <sub>3</sub> -N, kg/ha/yr	Mean retention of PO <sub>4</sub> -P, kg/ha/yr	Mean contribution of chlorophyll-a, kg/ha/yr
2	22.8%	8,690	564	13.8
6	4.7%	6,540	305	12.6
10	0.4%	2,980	97	32.8
12	0.1%	2,020	66	38.4

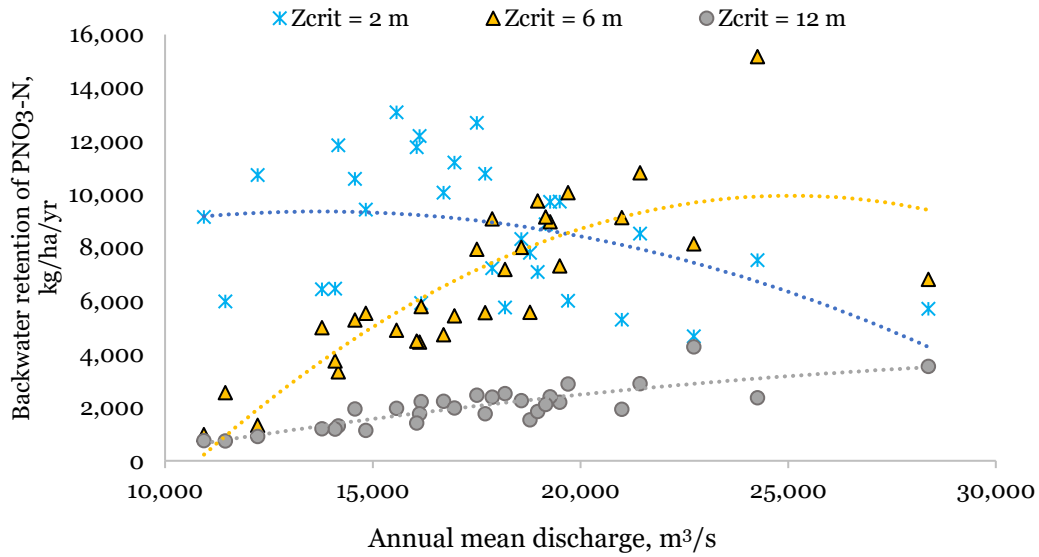


**Figure 3.** Annual mean retention of NO<sub>3</sub>-N by hypothetical backwater (**Table 1**) versus annual mean MC discharge for 1992-2021.

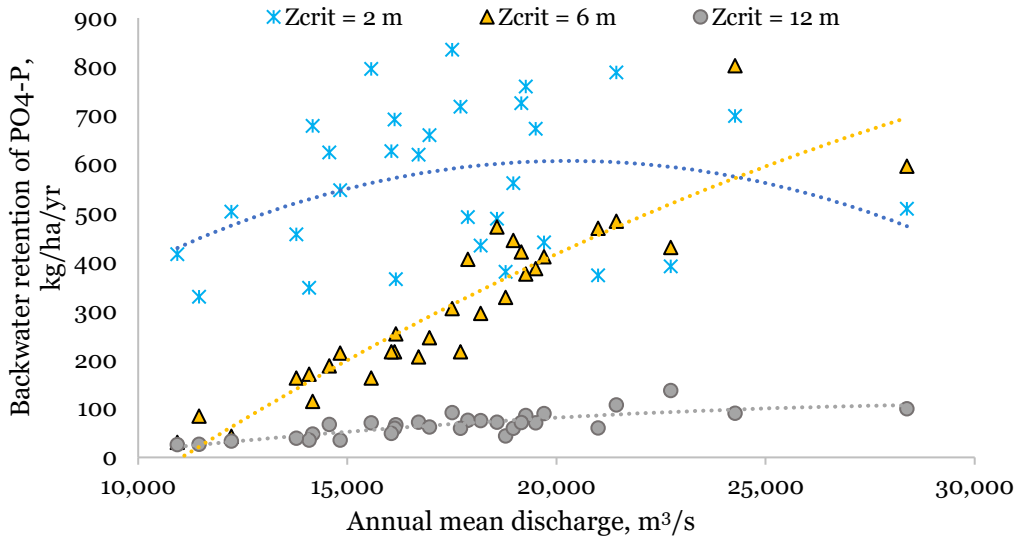


**Figure 4.** Annual mean retention of PO<sub>4</sub>-P by hypothetical backwater (**Table 1**) versus annual mean MC discharge for 1992-2021.

## Discussion

Stackpoole et al. (2021) estimated the annual load of NO<sub>3</sub> + NO<sub>2</sub> and PO<sub>4</sub>-P at the mouth of the Mississippi River between 1995 and 2017 to be about 900 kt and 50 kt, respectively. The values we computed for MC loads of NO<sub>3</sub>-N and PO<sub>4</sub>-P for our study reach for 1992-2021 (1,080 and 41 kt, respectively, **Table 5**) compared well with these values considering average flows at Helena were about 10% greater than those at Baton Rouge. Model output for 1995-2017 MC chlorophyll-a concentrations ( $8.5 \pm 2.6 \mu\text{g/L}$ ) are lower than reported by Turner et al. (2022) for 1997-2018 at Baton Rouge ( $13.8 \pm 0.2 \mu\text{g/L}$ ). Simulated rates of NO<sub>3</sub>-N retention per unit BW

area (~1,300-3,200 kg/ha/yr, **Table 6**) were an order of magnitude higher than NO<sub>3</sub>-N removal rates for inundated floodplains of North America and Europe presented in a review by Gordon et al. (2020) (mean = 200 kg/ha/yr, range = 2.35 to 962 kg NO<sub>3</sub>-N/ha/yr). Gordon et al. (2020) also found lower P reductions (mean = 21.0 kg/ha/yr, range -14.6 to 130 kg/ha/yr) than we did (~60-150 kg/ha/yr, **Table 6**). However, our figures are based on BW area rather than floodplain area, and this may account for some of the difference. Jacobson et al. (2022) estimated that the floodplain along the Lower Missouri River could potentially denitrify only 0.05%-1.7% of the mean annual N load, while we estimated that only the four LMR BW we simulated would retain an average of 0.34% of the LMR MC NO<sub>3</sub>-N load. However, Jacobson et al. (2022) based their estimates on floodplain (e.g., Gordon et al. 2020) rather than BW retention rates. We also estimated the four study BWs would retain an average of 0.39% of the PO<sub>4</sub>-P load and contribute 0.91% of the chlorophyll-a load.

Based on mean annual flow diversion, NO<sub>3</sub>-N retention in a given BW<sub>h</sub> increased with increasing levels of hydrologic connectivity (**Table 7, Figure 3**). Although conditions in disconnected (“isolated”) BWs are more favorable for biological uptake (algal blooms) and denitrification (anoxic conditions, plentiful organic carbon), the greater flux of NO<sub>3</sub>-N through the connected BW leads to greater retention (Jones et al. 2014). Retention of PO<sub>4</sub>-P displayed a similar relationship to BW connectivity (**Table 7, Figure 4**). Retention of PO<sub>4</sub>-P in isolated BWs may be mitigated by desorption of P from sediments under anoxic conditions (Jones et al. 2014, Justus 2022). The increasing variation in nutrient retention with increasing connectivity (**Figures 3 and 4**) may reflect the variation in hydrologic time series for each year and the greater influence of MC variation as connectivity increased. Further, as connectivity increased, nutrient retention declined when mean flows were very large because BW<sub>h</sub> was “flushed” and became increasingly similar to the MC.

Our results indicate modification of tie channels to increase the frequency and magnitude of flow-through connection between the LMR MC and BWs would enhance nutrient retention. However, retention may be subject to a host of site-specific factors which are not reflected in our simple model. Enlarging and maintaining tie channels to yield potential benefits would require solution of several engineering and environmental problems.

## Conclusions

The results of our empirical model application demonstrate the critical role that LMR BWs play in retaining excess nutrients and supporting primary production in the ecosystem. This finding highlights the importance of investing in the conservation, management, and protection of the remaining floodplains within the batture. Unfortunately, the construction of levees along the LMR has significantly reduced the functional BWs, underscoring the need for urgent action to preserve this vital resource.

Given the potential benefits of nutrient retention in BWs, we recommend further investigation through a more comprehensive study of selected BWs, supported by additional field data, state-of-the-art hydrodynamic modeling, and process-based water quality models. Such an approach would provide a more detailed understanding of nutrient retention dynamics in BWs, allowing for the development of more targeted conservation and management strategies.

It is critical to recognize that site-specific factors can impact BW processes, and our model does not account for all of these factors. Thus, the implementation of effective conservation and management strategies will require careful consideration of these factors in addition to our model's results. Nevertheless, our findings underscore the need for continued investment in the

preservation of LMR BWs to safeguard the ecosystem's health and ensure the sustainability of this important national and global resource.

## Acknowledgments

The US Army Corps of Engineers supported much of the work described herein through a cooperative agreement, FAIN W912HZ2020066. Billy Justus and Daniel Kroes read an earlier draft of this paper and made many helpful comments.

## References

- Alexander, R.B., Smith, R.A., and Schwarz, G.E. 2000. "Effect of stream channel size on the delivery of nitrogen to the Gulf of Mexico." *Nature*, 403, 758-761.
- Baker, J.A., Killgore, K.J., and Kasul, R.L. 1991. "Aquatic habitats and fish communities in the lower Mississippi River." *Aquatic Sciences*, 3, 313-353.
- Biedenbarn, D.S., Killgore, K.J., Little, C.D., Murphy, C.E. and Kleiss, B.A. 2018. "Attributes of the Lower Mississippi River Batture." *Mississippi River and Geomorphology and Potamology Program Technical Note No. 4*. Report prepared for the Mississippi River Commission. U.S. Army Corps of Engineers. Engineer Research and Development Center. Vicksburg, MS.
- Cloern, J.E. 2007. "Habitat connectivity and ecosystem productivity: implication from a simple model." *The American Naturalist*, 169, 21-33.
- Coupe, R.H., Goolsby, D.A., Battaglin, W.A., Böhlke, J.K., McMahon, P.B., and Kendall, C. 2013. "Transport of nitrate in the Mississippi River in July-August 1999." *Annals of Environmental Science*, 7, 31-46.
- Eckblad, J. W., Volden, C.S., and Weilgart, L.S. 1984. "Allochthonous drift from backwaters to the main channel of the Mississippi River." *American Midland Naturalist*, 111, 16-22.
- Evans, J.L., Murdock, J.N., Taylor, J.M. and Lizotte Jr, R.E. 2021. "Sediment Nutrient Flux Rates in a Shallow, Turbid Lake Are More Dependent on Water Quality Than Lake Depth." *Water*, 13(10), p.1344.
- Gagliano, S. M. and Howard, P. C. 1984. "The neck cutoff oxbow lake cycle along the Lower Mississippi River." In *River Meandering 1984* (pp. 147-158. American Society of Civil Engineers, Reston, VA.
- Goolsby, D. A., Battaglin, W.A., Lawrence, G.B., Artz, R.S., Aulenbach, B.T., Hooper, R.P., Keeney, D.R., and Stensland, G.J. 1999. "Flux and sources of nutrients in the Mississippi-Atchafalaya River Basin -topic 3, report for the integrated assessment of hypoxia in the Gulf of Mexico." NOAA Coastal Ocean Program.
- Gordon, B. A., Dorothy, O. and Lenhart, C. F. 2020. "Nutrient retention in ecologically functional floodplains: A review." *Water*, 12(10), 2762.
- Hartfield, P. 2014. "Engineered wildness." *International Journal of Wilderness*, 20, 8-13.
- Howe, E. M. and Gaines, R.A. 2017. "Hydraulic assessment of notched river training structures near Island 63 on the Lower Mississippi River." Draft Report, Mississippi River and Geomorphology and Potamology Program. U.S. Army Corps of Engineers. Vicksburg, MS.
- Jacobson, R. B., Bouska, K. L., Bulliner, E. A., Lindner, G. A. and Paukert, C. P. 2022. "Geomorphic Controls on Floodplain Connectivity, Ecosystem Services, and Sensitivity to Climate Change: An Example from the Lower Missouri River." *Water Resources Research*, 58(6), e2021WR031204.
- Jones, C. N., Scott, D. T. Edwards, B. L. and Keim, R. F. 2014. "Perirheic mixing and biogeochemical processing in flow-through and backwater floodplain wetlands." *Water Resour. Res.*, 50, 7394-7405, doi:10.1002/2014WR015647.
- Junk, W.J., Bayley, P.B., and Sparks, R.E. 1989. "The flood pulse concept in river-floodplain systems." In D.P. Dodge, (Ed.), *Proceedings of the International Large River Symposium*. Canadian Special Publication of Fisheries and Aquatic Sciences 106, 110-127.
- Justus, B.G., 2022. "Phosphorus Transport in the Mississippi Delta: Associations to Surface and Groundwater Interactions," *Water* 14, no. 18: 2925. <https://doi.org/10.3390/w14182925>
- Laurent, A. and Fennel, K. 2014. "Simulated reduction of hypoxia in the northern Gulf of Mexico due to phosphorus limitation." *Elementa: Science of the Anthropocene* 2: published online. <https://doi.org/10.12952/journal.elementa.000022>

- Miranda, L. E., Rhodes, M. C., Allen, Y., and Killgore, K. J. 2021. "An inventory and typology of permanent floodplain lakes in the Mississippi Alluvial Valley: a first step to conservation planning." *Aquatic Sciences*, 83(2), 1-11.
- Ochs, C.A., Pongruktham, O., and Zimba, P.V. 2013. "Darkness at the break of noon: Phytoplankton production in the Lower Mississippi River." *Limnology and Oceanography*, 58, 555-568.
- Ochs, C. A. and Shields Jr, F. D. 2019. "Fluxes of nutrients and primary production between the main channel and floodplain backwaters of the Lower Mississippi River—Development of a simulation model." *River Research and Applications*, 35(7), 979-988.
- Pongruktham, O., and Ochs, C.A. 2015. "The rise and fall of the Lower Mississippi: Effects of hydrologic connection on floodplain backwaters." *Hydrobiologia*, 742, 169-183.
- Richards, K. 1982. *Rivers Form and Process in alluvial channels*. Chapter 6, "The morphology of river cross sections." Methuen and Company., London and New York, NY.
- Rowland, J. C., Lepper, K., Dietrich, W. E., Wilson, C. J., and Sheldon, R. 2005. "Tie channel sedimentation rates, oxbow formation age and channel migration rate from optically stimulated luminescence (OSL) analysis of floodplain deposits." *Earth Surface Processes and Landforms: The Journal of the British Geomorphological Research Group*, 30(9), 1161-1179.
- Scott, D.T., Keim, R.F., Edwards, B.L., Jones, C.N., and Kroes, D.E. 2014. "Floodplain biogeochemical processing of floodwaters in the Atchafalaya River Basin during the Mississippi River flood of 2011." *Journal of Geophysical Research: Biogeosciences*, 119, 537-546.
- Schramm Jr, H.L., Cox, M.S., Tietjen, T.E., and Ezell, A.W. 2009. "Nutrient dynamics in the Lower Mississippi River floodplain: Comparing present and historic hydrologic conditions." *Wetlands* 29: 476-487.
- Shields Jr, F. D. 1995. "Fate of Lower Mississippi River habitats associated with river training dikes." *Aquatic Conservation: Marine and Freshwater Ecosystems*, 5(2), 97-108.
- Shields, F. D., Jr., and Abt, S. R. 1989. "Sediment deposition in cutoff meander bends and implications for effective management." *Regulated Rivers: Research and Management* 4:381-396.
- Strauss, E.A., Richardson, W.B., Bartsch, L.A., and Cavanaugh. 2011. "Effect of habitat type on in-stream nitrogen loss in the Mississippi River." *River Systems* 19, 261-269.
- Stackpoole, S., Sabo, R., Falcone, J., and Sprague, L.A. 2021. "Long-term Mississippi River trends expose shifts in the river load response to watershed nutrient balances between 1975 and 2017." *Water Resources Research* 57(11). Published Online at <https://doi.org/10.1029/2021WR030318>.
- Thackston, E. L., Shields Jr, F. D., and Schroeder, P. R. 1987. "Residence time distributions of shallow basins." *Journal of Environmental Engineering*, 113(6), 1319-1332.
- Tian, H., Xu, R., Pan, S., Yao, Y., Bian, Z., Cai, W.J., Hopkinson, C.S., Justic, D., Lohrenz, S., Lu, C., Ren, W., and Yang, J. 2020. "Long-term trajectory of nitrogen loading and delivery from Mississippi River Basin to the Gulf of Mexico." *Global Biogeochemical Cycles*, 34. Published Online.
- Turner, R. E., Milan, C. S., Swenson, E. M., & Lee, J. M. 2022. "Peak chlorophyll a concentrations in the lower Mississippi River from 1997 to 2018." *Limnology and Oceanography*, 67(3), 703-712. <https://doi.org/10.1002/lno.12030>
- U.S. Geological Survey (USGS). 2022. "USGS water data for the Nation: U.S. Geological Survey National Water Information System database." Retrieved from <http://waterdata.usgs.gov/nwis/>
- Withers, P. J. A. and Jarvie, H.P. 2008. "Delivery and cycling of phosphorus in rivers: A review." *Science of the Total Environment* 400(1-3): 379-395.
- Wohl, E. 2021. "An integrative conceptualization of floodplain storage." *Reviews of Geophysics* 59(2): 1-63.